06

Electron microscopy analysis of the „ plasma coating−substrate“ contact zone

© I.V. Baklushina[1], V.E. Gromov[1], Yu.F. Ivanov[2], I.Yu. Litovchenko[3], A.S. Chapaikin[1]

[1] Siberian State Industrial University, Novokuznetsk, Russia
[2] Institute of High Current Electronics, Siberian Branch, Russian Academy of Sciences, Tomsk, Russia
[3] Institute of Strength Physics and Materials Science, Siberian Branch, Russian Academy of Sciences, Tomsk, Russia
E-mail: gromov@physics.sibsiu.ru

Received June 25, 2025
Revised October 28, 2025
Accepted October 28, 2025

Using modern physical materials science methods, the structural-phase states and elemental composition of the transition zone in the „plasma coating (high-speed molybdenum steel)−substrate (medium-carbon steel)“ system were investigated. It was found that the transition layer, approximately 100 micrometers thick, contains α-phase, γ-phase, complex carbides ($M_{23}C_6$, M_6C), as well as MoC and cementite.

Keywords: high-speed molybdenum steel, „plasma coating−substrate“ system, contact zone, structure, phase composition

DOI: 10.61011/TPL.2026.02.63047.20416

To increase the wear resistance of working surfaces of mechanisms, machines, and structures operating under extreme conditions, plasma surfacing is performed with the use of modern surfacing materials [1–3] and nitrogen serving as an alloying and shielding element, which provides an additional significant increase in operational properties [4–6]. The use of high-speed steels in resource- and energy-saving plasma surfacing technologies satisfies the stringent requirements of mechanical engineering, metallurgy, mining, and other industries [7,8].

The last quarter of the 20th century was marked by the widespread use of high-speed steels containing 8–10 wt.% molybdenum [9]. Compared to tungsten, this element is less scarce and expensive, but provides better functional properties [10–12].

The issue of state of the coating–substrate transition zone remains relevant in coating research, since the damping and adhesive properties of this material volume are crucial for reliable operation of coated machine parts, mechanisms, and structures [13,14]. Only a few papers focused on this topic have been published in Russia and abroad, which limits the practical application of high-speed molybdenum steel coatings.

In view of this, the present study is aimed at examining the structure and properties of the interface of the coating−substrate system formed by the plasma method.

Research samples were obtained by plasma surfacing of 30KhGSA steel in a nitrogen environment. The overlay layer formation parameters were as follows: welding current, 145−150 A; arc voltage, 50−55 V; deposition rate, 18 m/h; wire feed rate, 60 m/h; arc length, 20 mm.

A MoCrCoC flux-cored wire with a diameter of 4 mm was used to form an overlay $\sim$ 9 mm in thickness.

The chemical composition of 30KhGSA steel (wt.%) is as follows: C — 0.3; Cr — 0.9; Mn — 0.8; Si — 0.9; the rest is Fe. The chemical composition of the overlay corresponds to SAE-AISI M9 (T11309) molybdenum high-speed steel (wt.%): C — 1−1.1; Mo — 8.85; Cr — 3.57; Co — 2.12; V — 0.05; Si — 1.12; Mn — 0.56; Al — 1.05; the rest is Fe. High-grade argon (GOST 10157−79) with a flow rate of 0.1−0.13 l/s was used as a plasma-forming

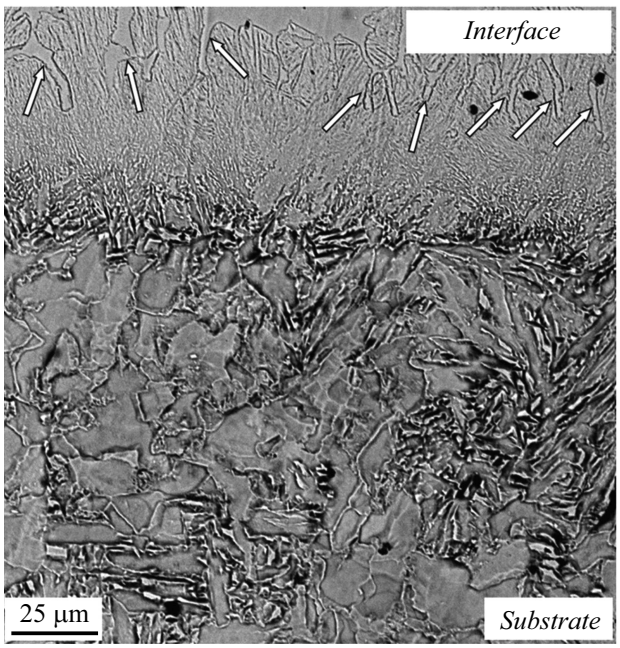

Figure 1. Structure of the transition layer formed as a result of depositing M9 steel onto 30KhGSA steel. Scanning electron microscopy image of an etched slice. Arrows indicate eutectic interlayers.

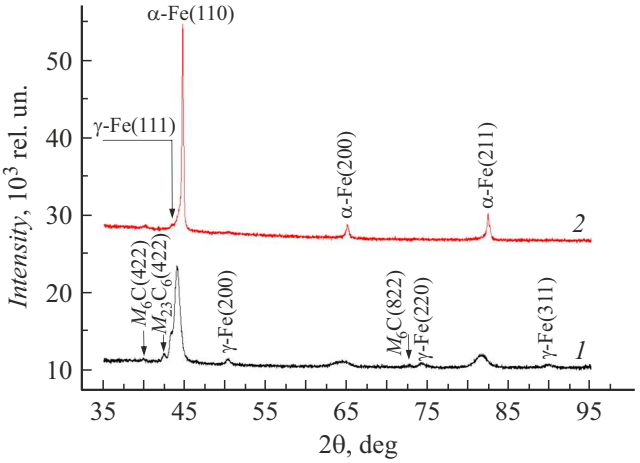

Figure 2. Fragments of X-ray diffraction patterns of the M9 steel overlay (*1*) and the interface of the overlay (M9)/substrate (30KhGSA steel) system (*2*).

gas; technically pure nitrogen (GOST 9293–74) with a flow rate of 0.3–0.4 l/s was the shielding and alloying gas. The regimes of plasma surfacing at a UD-417 setup were the same as those detailed in [13,14].

The phase composition of the coating–substrate system was studied by X-ray diffraction analysis using a DRON-8N diffractometer.

Identification of the phase composition, qualitative and quantitative phase analysis, and refinement of the structure parameters were performed using the CDA (Crystallography and Diffraction Analysis) software package with a built-in catalogue of powder standards (AO Burevestnik, version 2023-01-24-144022.8dec10c0f). The structure and elemental composition of the coating–substrate system were examined with a KYKY-EM6900 scanning electron microscope (SEM). The defect substructure and elemental and phase composition of the coating–substrate system were studied using transmission electron diffraction microscopy (TEM) of thin foils in transmission and scanning modes (JEOL JEM-2100 device, Japan) [15–17].

SEM images of an etched slice revealed that plasma surfacing is accompanied by the formation of a transition layer with a thickness up to 100 μm and a structure differing from the state of steel in the bulk of the overlay (Fig. 1). X-ray microanalysis demonstrated that, in addition to chemical elements of the wire used to form the surface layer, oxygen atoms are present in the transition layer of the coating–substrate system. This is apparently indicative of the presence of oxygen atoms on the surface (in the surface layer) of the substrate. It should be noted that the relative concentration of alloying elements (Al, Cr, Co, Mo) decreases as one approaches the transition layer from the side of the overlay, while the concentration of Si and Mn increases.

Visualization (mapping) of the elemental distribution of the coating–substrate system revealed that molybdenum and chromium atoms are concentrated predominantly in the surface coating, while the transition layer is enriched with aluminum and oxygen atoms, which apparently form aluminum oxides. This may be attributed to a suboptimal quality of preparation of the substrate surface after grinding with corundum. The substrate layer adjacent to the transition layer is enriched with oxygen atoms.

The results of X-ray diffraction analysis are indicative of the formation of a multiphase structure in the overlay, which contains α and γ phases, carbides of a complex composition

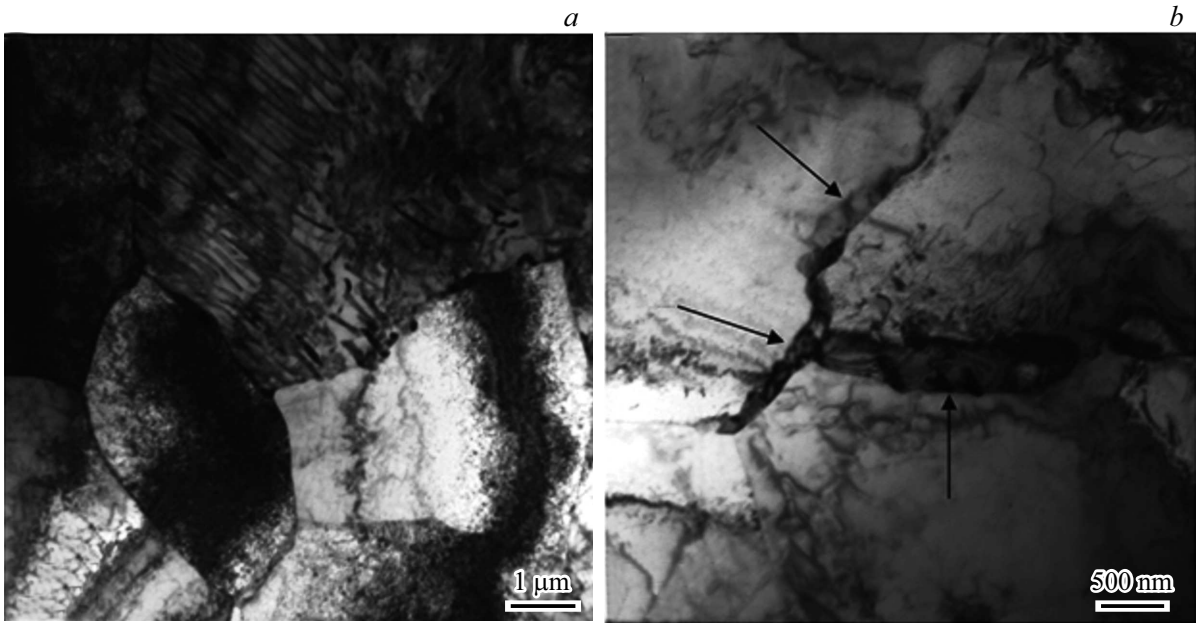

Figure 3. TEM image of the substrate structure in the zone of contact with deposited metal. *a* — Micrometer-sized ferrite grains; *b* — second-phase interlayers along the grain boundaries (interlayers are indicated by arrows).

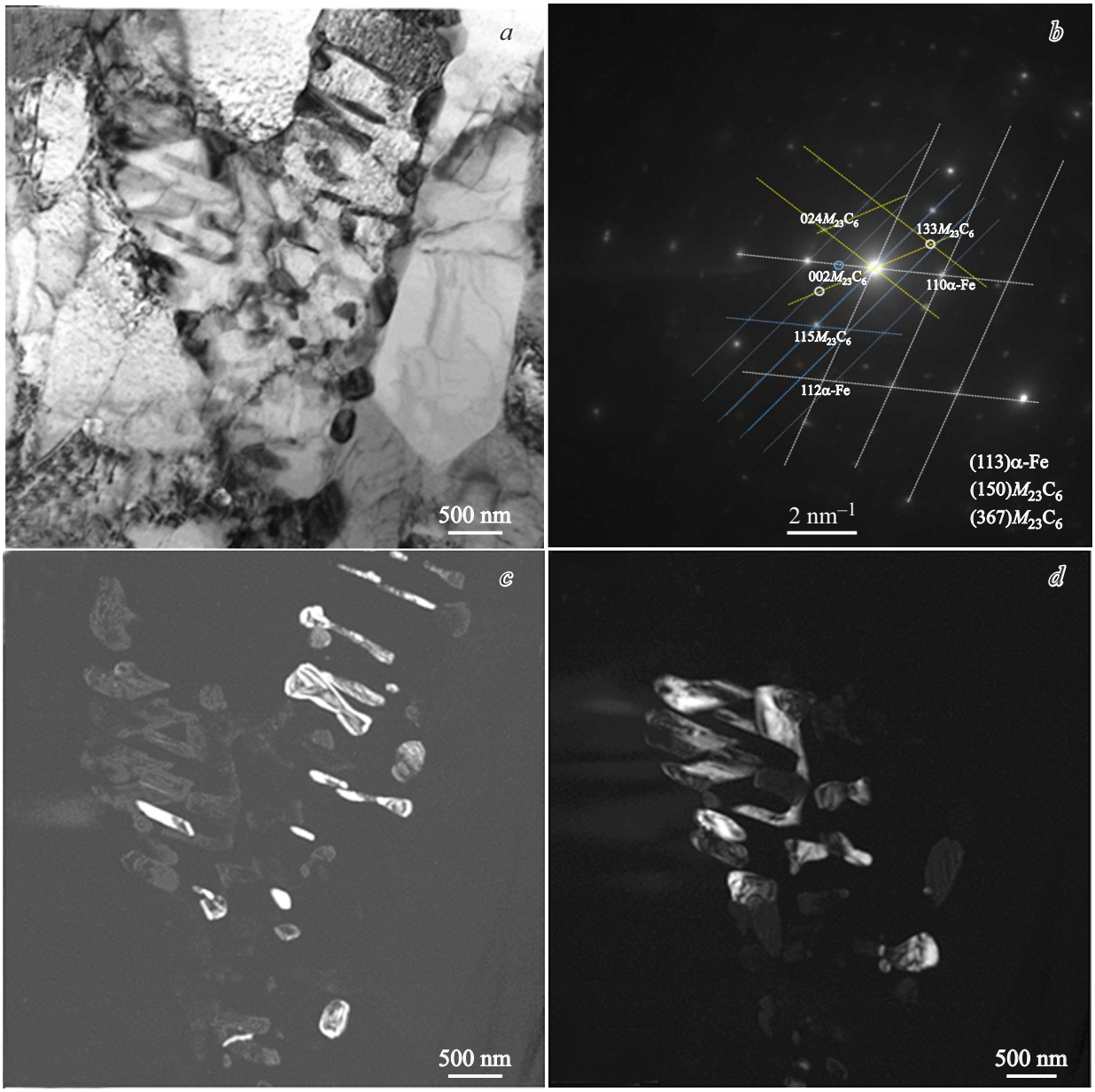

Figure 4. TEM image of the interface structure of the coating–substrate system. *a* — Bright field; *b* — electron microdiffraction pattern; *c*, *d* — dark-field images in reflections (024) $M_{23}C_6$ + (103) η-MoC (*c*) and (115) $M_{23}C_6$ (*d*).

($M_{23}C_6$ and M_6C), and iron carbide Fe_2C (Fig. 2). As was expected, the primary phase is a solid solution based on α-Fe (65 wt.%). The amount of a solid solution based on γ-Fe (12 wt.%) is significantly lower, and the relative content of carbide phases reaches 23 wt.% (with carbides of complex compositions $M_{23}C_6$ and M_6C being dominant). It should be noted that the parameters of crystal lattices of the α and γ phases exceed significantly the tabular values of parameters of crystal lattices of α- and γ-Fe [18]. This is indicative of the formation of iron-based substitution and interstitial solid solutions in the overlay. According to the results of X-ray diffraction analysis, the α phase is, as expected, the primary phase of the transition layer; small amounts of the γ phase and complex carbide M_6C are also present.

Scanning electron microscopy revealed no micropores or microcracks in the coating–substrate contact zone. The substrate (30KhGSA steel) has a polycrystalline structure with ferrite grains and pearlite grains of a lamellar morphology. The grain size varies within the 5.2–12.3 μm range. It should be noted that the transition layer directly adjacent to the contact zone has a lamellar structure, which may be indicative of a shear (martensitic or bainitic) mechanism for the formation of this material region. At a greater distance from the contact zone, extended interlayers emerge in the transition layer.

The study of elemental and phase composition, phase morphology, and defect substructure by transmission electron diffraction microscopy confirmed that the substrate structure is formed by pearlite and ferrite grains. Pearlite has a lamellar morphology and is formed by alternating layers of cementite and α-Fe.

A lamellar structure is observed in the transition layer grains, which is indicative of martensitic nature of formation of the α phase structure. Extended interlayers with a structure characteristic of a eutectic transformation are observed along the grain boundaries.

In the contact zone on the substrate side, the structure retains its ferrite–pearlite state, but the size of ferrite grains is reduced significantly (down to $1.5-2.3\,\mu$m; see Fig. 3, *a*). Extended interlayers of the second phase (marked by arrows in Fig. 3, *b*) are seen along the grain boundaries. Transmission electron diffraction microscopy revealed that the transition layer lamellae were formed by a shear mechanism; based on morphological features, they were identified as lamellar and packet martensite. Nanosized ($15-32$ nm) particles of iron carbide (cementite) are located along the boundaries of lamellae and packets. At the same time, extended interlayers of residual austenite are positioned along the boundaries of martensite crystals. Thus, a multiphase structure is formed during surfacing in the transition layer in the contact zone on the substrate side. Its components are martensite, residual austenite, and iron carbides.

The transition layer directly adjacent to the overlay contains extended interlayers with inclusions of the second phase (Fig. 3, *b*): α phase and M_6C, $M_{23}C_6$, and MoC carbides (Fig. 4). It is fair to assume that these layers were formed by the eutectic mechanism in the process of crystallization of molten metal of the coating.

Thus, the obtained results suggest that the formation of the overlay is accompanied by the emergence of a transition layer with a thickness up to $100\,\mu$m and a multiphase structure containing the primary α phase; residual austenite; cementite particles; and M_6C, $M_{23}C_6$, and MoC carbides.

It was established that the high-speed molybdenum steel coating produced by plasma surfacing has a polycrystalline structure and is formed by grains based on the α phase and eutectic grains. Its formation is accompanied by the emergence of a transition layer with a thickness up to $100\,\mu$m. It was demonstrated that the primary phase in the transition layer directly adjacent to the overlay is the α phase; a small amount of the γ phase, complex carbides M_6C and $M_{23}C_6$, MoC, and cementite are also present. It was found that the transition layer in the contact zone on the substrate side has a hardened structure with lamellae and packets of martensite, layers of residual austenite, and nanosized cementite particles. It was established that the coating–substrate contact zone does not contain microcracks and micropores.

The structural-phase state and elemental composition of the interface of the plasma coating (high-speed molybdenum steel)–substrate (medium-carbon steel) system, which have been determined for the first time, are indicative of a high performance efficiency of this system and bright prospects of its practical application.

Funding

This study was supported by grant No.23-19-00186 from the Russian Science Foundation (https://rscf.ru/project/23-19-00186).

Conflict of interest

The authors declare that they have no conflict of interest.

References

[1] A.N. Emelyushin, E.V. Petrochenko, S. P. Nefed'ev, Weld. Int., **27** (2), 150 (2012). DOI: 10.1080/09507116.2012.695548
[2] I.V. Mozgovoi, E.A. Shneider, *Naplavka bystrorezhushchei stali* (Izd. Omsk. Gos. Tekh. Univ., Omsk, 2016) (in Russian).
[3] Y.F. Ivanov, V.E. Gromov, A.I. Potekaev, T.P. Guseva, A.S. Chapaikin, E.S. Vashchuk, D.A. Romanov, Russ. Phys. J., **66** (7), 731 (2023). DOI: 10.1007/s11182-023-02999-w
[4] S.P. Nefed'ev, A.N. Emelyushin, Vestn. Yugorsk. Gos. Univ., No. 3 (62), 33 (2021) (in Russian). DOI: 10.17816/byusu20210333-45
[5] A.N. Emelyushin, E.V. Petrochenko, S.P. Nefed'ev, Svar. Proizvod., No. 10, 18 (2011) (in Russian).
[6] S.P. Nefed'ev, A.N. Emelyushin, *Plazmennoe uprochnenie poverkhnosti detalei* (TNT, Staryi Oskol, 2021) (in Russian).
[7] L.S. Kremnev, A.K. Onegina, L.A. Vinogradova, Metalloved. Term. Obrab. Met., No. 12 (654), 13 (2009) (in Russian).
[8] L.S. Kremnev, Metalloved. Term. Obrab. Met., No. 11, 18 (2008) (in Russian).
[9] V.E. Gromov, A.S. Chapaikin, S.A. Nevskii, *Struktura, svoistva i modeli naplavki bystrorezhushchei stali posle otpuska i elektronno-puchkovoi obrabotki* (Poligrafist, Novokuznetsk, 2024) (in Russian).
[10] I.K. Kupalova, Zavod. Lab., No. 1, 27 (1983) (in Russian).
[11] Yu.F. Ivanov, *Strukturnye i fazovye prevrashcheniya v ryade stalei pri staticheskom i dinamicheskom rezhimakh termicheskoi obrabotki*, Doctoral Dissertation in Mathematics and Physics (Inst. Phys. Strength Mater. Sci., Tomsk, 2002) (in Russian).
[12] V.P. Rotshtein, D.I. Proskurovskii, G.E. Ozur, Yu.F. Ivanov, *Modifikatsiya poverkhnosti metallicheskikh materialov nizkoenergeticheskimi sil'notochnymi elektronnymi puchkami* (Nauka, Novosibirsk, 2019) (in Russian).
[13] V.E. Gromov, A.B. Yur'ev, YU.F. Ivanov, S.S. Minenko, S.V. Konovalov, Vestn. Sib. Gos. Ind. Univ., No. 2 (52), 9 (2025) (in Russian). DOI: 10.57070/2304-4497-2025-2(52)-9-16
[14] A.I. Potekaev, V.E. Gromov, A.B. Yuriev, Yu.F. Ivanov, S.V. Konovalov, S.S. Minenko, A.P. Semin, A.S. Chapaikin, I.Yu. Litovchenko, Russ. Phys. J., **67** (8), 1107 (2024). DOI: 10.1007/s11182-024-03222-0
[15] F.R. Egerton, *Physical principles of electron microscopy* (Springer International Publ., Basel, 2016).

[16] C.S.S.R. Kumar, *Transmission electron microscopy. Characterization of nanomaterials* (Springer, N.Y., 2014).
[17] C.B. Carter, D.B. Williams, *Transmission electron microscopy* (Springer International Publ., Berlin, 2016).
[18] V.G. Kurdyumov, L.M. Utevskii, R.I. Entin, *Prevrashcheniya v zheleze i stali* (Nauka, M., 1977) (in Russian).

Translated by D.Safin